I&EC research
Industrial & Engineering Chemistry Research

Article

Cite This: Ind. Eng. Chem. Res. 2018, 57, 1679−1688

pubs.acs.org/IECR

Modeling Thermodynamic Properties of Isomeric Alkanes with a New Branched Equation of State

Yuchong Zhang and Walter G. Chapman*

Department of Chemical and Biomolecular Engineering, Rice University, Houston, Texas 77005, United States

ABSTRACT: In this paper we present an extension of the statistical associating fluid theory (SAFT) for branched molecules with a Lennard-Jones dimer reference fluid (SAFTD-LJ-Branch). The theory successfully predicts how branched architecture affects the attraction and repulsion between molecules. SAFTD-LJ-Branch takes a form similar to SAFTD-LJ with an additional parameter NB introduced to account for the branching effect. We propose an approach relating NB to the number of different types of articulation segments. The theory is used to study the effect of chain architecture on the thermodynamic properties of isomeric alkanes. SAFTD-LJ-Branch accurately predicts the phase diagram of pure butane, pentane or hexane isomers. Further, vapor pressures of *n*-triacontane and squalane are predicted without further fitting and shown to be in semiquantitative agreement with experimental data. Finally, SAFTD-LJ-Branch is demonstrated to be well applicable to mixtures as we model the vapor−liquid coexistence of binary alkane mixtures containing different hexane isomers and recover the experimental trends.

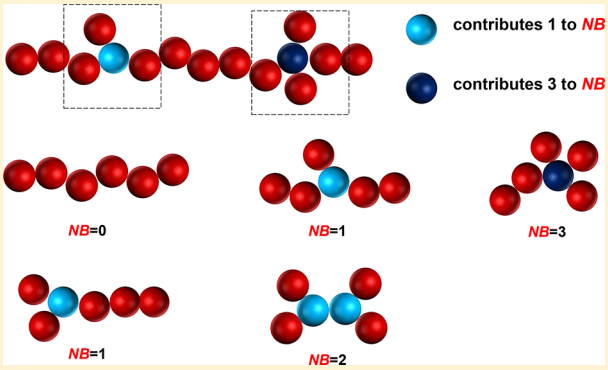

1. INTRODUCTION

Molecular architecture affects the phase behavior of polyatomic molecules.[1] Energetically, the intermolecular interactions between atoms or groups can be shielded due to the addition of branches. From the entropic respect, different favored conformations might be assumed for different molecular structures.[2] All these factors lead to a difference in phase change and fluid structure as well as other thermodynamic properties in a complex way.[3−6] However, whether it is short chains or long polymers, any property change due to branching matters for industrial processing. The effects of molecular architecture on thermodynamic properties are obtained primarily from experiments, which are expensive and time-consuming. It is impossible to consider the full range of state points and branched structures only from experiments. Practicing engineers many times must estimate fluid properties for components lacking experimental data. This is sometimes done by comparing with reference components that differ in molecular architecture. Therefore, a theoretical model that accurately predicts the effect of branching on thermodynamic properties is needed.

One popular theory to describe how molecular structure affects fluid properties, is lattice cluster theory (LCT), originally developed by Freed et al.[7,8] and extended to compressible systems by Dudowicz et al.[9,10] LCT uses a double series expansion in the inverse coordination number and the reduced interaction energy to arrive at the free energy of a structured lattice fluid characterized by several combinatorial numbers giving the number of distinct ways to find a given substructure in the molecular architecture of the fluid under consideration. It has been tested against lattice Monte Carlo simulation[11] and extended to include semiflexibility and association interactions in the same lattice formalism.[12] Especially the group of Enders has applied it successfully for polymeric and nonpolymeric systems.[13−20] However, as a lattice theory, LCT sometimes performs weakly for the gas phase. Also the selection of the lattice coordination number can be quite empirical for off-lattice applications.

Another successful category of models is perturbation theory, particularly, the statistical associating fluid theory (SAFT) equation of state (EoS).[21−25] SAFT models molecules as chains of spherical segments. It lays its foundation on Wertheim's first-order thermodynamic perturbation theory (TPT1),[26−29] which is a rigorous statistical mechanical theory of associating spheres. The excess Helmholtz free energy of a system can be viewed as a sum of the reference fluid contribution plus contributions from chain formation, association, dispersion, and other interactions. The perturbation expansion is typically written for a hard sphere reference fluid,[21] Lennard-Jones reference fluid[30] or square well fluid.[31] Depending on the applied interaction potential, different versions of SAFT have been developed, such as PC-SAFT,[32,33] Soft-SAFT,[34] and SAFT-VR.[35]

In TPT1, only pair correlations are included in the cluster expansion for association or chain formation. Therefore, interactions between non-nearest neighbors are neglected. As a result, all the major versions of SAFT EoS are implicitly

Received: September 22, 2017
Revised: December 1, 2017
Accepted: January 4, 2018
Published: January 4, 2018

DOI: 10.1021/acs.iecr.7b03951
Ind. Eng. Chem. Res. 2018, 57, 1679−1688

developed for linear chains. To explicitly include the structural information in the SAFT EoS, a higher level of perturbation theory must be considered, at least a second-order perturbation (TPT2).[36] TPT2 was extended from TPT1 by Wertheim,[36] where all graphs with a single path of two attraction bonds are retained in addition to the graphs retained in TPT1, thus providing information between bonded pairs and next nearest neighbors along the chain. TPT2 differs from TPT1 by a small term and achieves improved agreement with simulation results. Phan et al.[37] first derived a TPT2 equation of state for hard sphere chains, including star-like molecules. They were able to predict the pressure of freely rotating chains and that of trimers as a function of the bond angle. Marshall and Chapman[38] extended this approach further to generate a TPT2 correction for any branched molecule. However, it is challenging to evaluate the TPT2 contributions in the above equations of state.

Besides referring to TPT2, another strategy to improve the behavior of the SAFT EoS is using a fluid of dimers as a reference fluid. The dimers consist of two spheres bonded at contact, and it is assumed that the correlation function for longer chains can be approximated by the dimer correlation function. As a result, in this dimer scheme, a segment knows the information on nearest neighbor and also the next nearest neighbor. The first SAFT-D was independently developed by Ghonasgi and Chapman[39−42] and by Chang and Sandler[43] with the reference fluid being hard sphere dimers. With the same strategy, the Lennard-Jones (LJ) reference fluid can also be extended to LJ dimer and Johnson[44] used it to predict thermodynamics of pure components. Later, Blas and Vega[45] also demonstrated that Soft-SAFT-D could be applied to mixtures with improvement over Soft-SAFT, which basically uses LJ spheres as the reference fluid. Despite the improvement over the monomer version, no branching effect is taken into consideration for the dimer version.

Recently, Marshall and Chapman[46] proposed a different approach to construct the second-order correction to the free energy for branched molecules and showed that a similar form of correction can be applied in a TPT1-D type of equation of state. Specifically, a correction to SAFTD-LJ will yield a new equation of state that not only maintains a simple analytic form but also directly applies to real components. In this work, we follow similar lines and find it possible to further modify the correction to improve predictions for real systems. We name this equation of state SAFTD-LJ-Branch. We have used SAFTD-LJ-Branch to systematically study the phase behavior of alkane isomers. The phase diagram and vapor pressures of pure isomeric alkanes as well as vapor liquid equilibria (VLE) of alkane mixtures are modeled. The theoretical predictions agree well with experimental data, validating the new equation of state.

The paper is organized as follows. In section 2, SAFTD-LJ-Branch is developed for branched molecules. In section 3, parameters are fitted, correlated, and validated. Alkane systems of interest are studied with the application of SAFTD-LJ-Branch.

2. THEORY

In this section, we introduce SAFTD-LJ[44] and then include the branch correction to obtain SAFTD-LJ-Branch. Finally, the conventional van der Waals one-fluid mixing rules (VdW1)[47] are applied for extension to mixtures.

2.1. Formalism of SAFTD-LJ. In the scheme of SAFTD-LJ, if no association exists, the residual Helmholtz free energy of a system can be written as the sum of LJ sphere free energy and chain formation free energy.

$$A_{res} = A_s + A_{chain} \tag{1}$$

Three parameters are needed in this model, that is, the number of spherical LJ segments in a molecule m, dispersion energy between LJ segments ϵ, and segment diameter σ. ϵ and σ are explicitly included in the LJ potential.

$$u_{LJ}(r) = 4\epsilon\left[\left(\frac{\sigma}{r}\right)^{12} - \left(\frac{\sigma}{r}\right)^{6}\right] \tag{2}$$

The term A_s accounts for the contribution from Lennard-Jones segments, and the term A_{chain} accounts for the contribution from the effect of segments connected into dimers and then chains of fixed number. We also define ρ as number density, N as number of chain molecules or segments, V as volume, T as temperature, p as pressure, and μ as chemical potential. The subscripts s and c refer to segment and chain, respectively. In the following formulas, all the quantities will be expressed in reduced forms as below:

$$\rho^* = \rho\sigma^3 = \frac{N}{V}\sigma^3,\ T^* = \frac{kT}{\epsilon},\ p^* = \frac{p\sigma^3}{\epsilon},\ A^* = \frac{A}{NkT},\ \mu^* = \frac{\mu}{kT}$$

Now we have the reduced residual Helmholtz free energy.

$$A^*_{res} = mA^*_s + A^*_{chain} \tag{3}$$

Note that the existence of m is due to the fact that A^*_s is reduced with the number of segments and A^*_{res} and A^*_{chain} are reduced with the number of chains. A^*_s is proposed by Johnson et al.[48] through correlations of simulation results, and its expression can be found in the Appendix. A^*_{chain} is expressed as[44,45]

$$A^*_{chain} = \frac{A_{chain}}{N_c kT} = -\frac{m}{2}\ln[g_s(\sigma)] + \left(1 - \frac{m}{2}\right)\ln[g_d(\sigma)] \tag{4}$$

where g_s and g_d are the pair radial distribution function of LJ spheres and the site−site distribution function of LJ dimers, respectively. Expressions for g_s and g_d at contact are also obtained from correlations fit to molecular simulation;[44,49] see details in the Appendix.

2.2. Formalism of SAFTD-LJ-Branch. Because the term A_s has no dependence on how the LJ spheres are connected and arranged, to account for branching, we focus on the chain formation term A_{chain}.

The reduced chain term in SAFTD-LJ can also be written as

$$A^*_{chain} = \frac{A_{chain}}{N_c kT} = (1 - m)\ln[g_s(\sigma)] - \left(\frac{m-2}{2}\right)\ln\left[\frac{g_d(\sigma)}{g_s(\sigma)}\right] \tag{5}$$

The first term in the bracket is the chain contribution in SAFT-LJ,[30,49−51] and the second term is a correction term to incorporate structural information for dimers. If there is no difference between the LJ sphere correlation function and LJ dimer correlation function, then this term vanishes. In SAFTD-LJ, a segment knows not only its nearest neighbor but also the next nearest neighbor. Thus, this term should be proportional to the number of three consecutive segments that can be found in the chain. For a linear chain with m segments, this number is

DOI: 10.1021/acs.iecr.7b03951
Ind. Eng. Chem. Res. 2018, 57, 1679−1688

$m - 2$. For branched chains, we come up with a way to determine this number through observation of articulation segments, that is, the segments with three or more arms. Figure 1a is a branched chain with six segments and there are two

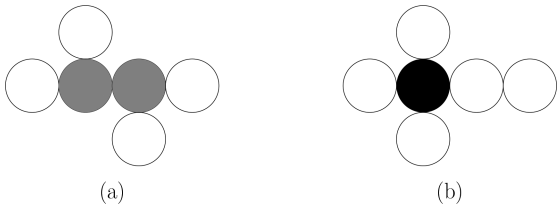

Figure 1. Molecules consisting of six segments but with different structures. Molecule a has two three-arm articulation segments (gray) and molecule b has one four-arm articulation segment (black). Each gray segment receives an NB = 1 and the black segment receives an NB = 3.

three-arm articulation segments, colored gray. The number of three consecutive segments is 6. However, Figure 1b is also a branched chain with six segments and there is one four-arm articulation segment, colored black. The number of three consecutive segments is 7. Generalizing to a branched chain with m segments, we introduce a new parameter NB to reflect the difference in the number of three consecutive segments compared with that of linear isomer (which is $m - 2$). By rule, a three-arm articulation segment contributes 1 to NB and a four-arm articulation segment contributes 3 to NB. For molecules with multiple articulation segments, NB is additive. Actually, this methodology can also be applied to articulation segments with more arms. However, for the molecules we are most interested in, such as alkanes, the inclusion of three-arm and four-arm articulation segments are enough.

On the basis of this analysis, we develop a new chain term that takes branched structure into consideration.

$$A^*_{\text{chain}} = \frac{A_{\text{chain}}}{N_c kT} = (1 - m)\ln[g_s(\sigma)] - \left(\frac{m - 2 + \text{NB}}{2}\right) \ln\left[\frac{g_d(\sigma)}{g_s(\sigma)}\right] \tag{6}$$

When NB = 0, this term is the same as eq 5, meaning that SAFTD-LJ-Branch simply reduces to SAFTD-LJ for linear chains. This expression is the same as proposed by Marshall and Chapman.[46] They applied the theory to branched alkanes, but not to mixtures.

It is interesting to note that the architecture in LCT is accounted for by a series of combinatorial numbers,[12,18] the number of segments m, the number of bonds $m - 1$, the number of two consecutive bonds N_2, and the number of three consecutive bonds N_3. The impact of architecture on thermodynamics arises starting with the occurrence of N_2 in the series expansion of LCT, which is on the same level of approximation as our expression $m - 2 + \text{NB}$. This similarity between the two theories is especially striking, because they are derived in a completely different formalism. This strengthens both theoretical results to some extent and it would be interesting to see, if further similarities occur, once trimer and tetramer correlation functions are available.

The resulting SAFTD-LJ-Branch, has four parameters in total, that is, m, σ, ϵ, and NB. We assume that to model isomers with different branching structures, m, σ, and ϵ can be kept the same and the only different parameter is NB. This assumption allows us to predict the phase behavior of numerous chemicals from data for isomers. The approach should be applicable to isomers with similar numbers and types of functional groups, such as alkanes and primary alcohols.

2.3. VdW1 Theory for Mixtures. Like other SAFT equations of states, SAFTD-LJ-Branch can be easily extended to mixtures with the approximation of van der Waals One-Fluid Theory,[47] which is a well-established conformal solution theory. VdW1 defines parameters of a hypothetical pure fluid x having the same residual properties as the mixture of interest. For σ_x and ϵ_x, the mixing rules are

$$\sigma_x^3 = \frac{\sum_i \sum_j m_i m_j x_i x_j \sigma_{ij}^3}{\sum_i \sum_j m_i m_j x_i x_j} \tag{7}$$

$$\epsilon_x \sigma_x^3 = \frac{\sum_i \sum_j m_i m_j x_i x_j \epsilon_{ij} \sigma_{ij}^3}{\sum_i \sum_j m_i m_j x_i x_j} \tag{8}$$

$$\sigma_{ij} = \frac{\sigma_{ii} + \sigma_{jj}}{2} \qquad \epsilon_{ij} = \sqrt{\epsilon_{ii}\epsilon_{jj}} \tag{9}$$

where x_i is the mole fraction of component i.

The effective segment number or branching parameter of the conformal fluid is simply the average segment number or branching parameter of the mixture.

$$m_x = \sum_i m_i x_i \qquad \text{NB}_x = \sum_i \text{NB}_i x_i \tag{10}$$

3. RESULTS AND DISCUSSION

Despite their simplicity compared to other molecules, the alkane families are of importance across many industries. The thermodynamic properties of even light alkane isomers are difficult to predict from existing models. Therefore, we focus on the phase behavior of alkane isomers to test the accuracy of SAFTD-LJ-Branch. The following results begin with fitting and correlation of parameters, and then SAFTD-LJ-Branch is applied to pure components as well as alkane mixtures.

3.1. Parameters for Pure Normal Alkanes. As mentioned before, SAFTD-LJ-Branch simply reduces to SAFTD-LJ for linear chains with NB = 0 and we should have the same parameters (m, σ, and ϵ) for the two equations of state. However, previous works with SAFTD-LJ[44,45] mainly consider a LJ model fluid and no parameters are available for real components. Therefore, we started by fitting parameters for normal alkanes from C_3 to C_{10}. During the fitting process, m, σ, and ϵ are fitted at the same time to vapor pressure (p_V) and liquid molar volume (v_L) data of pure components[52] within the temperature range of interest. The fitting results are presented in Table. 1.

The equation of state parameters are plotted versus molecular weight (MW) of n-alkanes starting from propane in Figure 2.

We see that the plots of all three parameters show a smooth trend. Inspired by Pedrosa et al.,[53] we succeed in correlating the parameters with molecular weight with the following expressions.

$$m = 0.0248\text{MW} + 0.8063 \tag{11a}$$

$$m\sigma^3 = 1.7437\text{MW} + 23.469 \tag{11b}$$

DOI: 10.1021/acs.iecr.7b03951
Ind. Eng. Chem. Res. 2018, 57, 1679−1688

Table 1. Pure Component Parameters for Normal Alkanes from C_3 to C_{10}

carbon no.	m	σ [Å]	ϵ/k [K]	AAD (p_V) [%]	AAD (v_L) [%]	T range [K]
3	1.913	3.726	214.3	0.535	0.495	200−350
4	2.249	3.819	232.1	1.256	2.076	195−420
5	2.581	3.874	245.3	0.877	1.566	220−460
6	2.941	3.904	253.9	1.057	1.817	250−500
7	3.276	3.926	261.8	0.628	0.814	229−501
8	3.651	3.933	266.7	0.859	0.611	254−526
9	3.993	3.953	271.5	0.990	0.583	266−554
10	4.335	3.971	275.3	0.868	0.570	286−574

$$\epsilon/k = \frac{314.998\mathrm{MW} - 209.288}{\mathrm{MW} + 19.7705} \tag{11c}$$

3.2. Phase Equilibrium of Pure Isomeric Alkane.

3.2.1. VLE of n-Alkanes versus Isoalkanes. In the frame of SAFTD-LJ-Branch, isomeric alkanes share the same parameters except for NB, which is related to the structure of a molecule and determined by the numbers of different types of articulation points.

As a first examination, we model vapor liquid equilibrium for *n*-alkanes and their corresponding isoalkane isomers. In Figure 3, the predictions for butane, pentane, and hexane are compared against NIST values,[52] which are correlations of experimental data. We observe overall good agreement. The model does extremely well in predicting vapor density and vapor pressure whereas it underestimates the branching effect on liquid density. Table 2 shows the average absolute deviations for predictions of vapor pressure and liquid molar volume in the investigated temperature range. In agreement with experiment, we find that isoalkanes tend to have a higher critical density and a lower critical temperature than its linear isomer. The error in critical temperature can be corrected by including fluctuation.[54] Significant deviations are expected if the molecular structure becomes spherical, such as isobutane. This is because the branching effect is accounted for on the basis of a linear chain model, and increasing sphericity introduces unanticipated symmetry, which affects the thermodynamics of molecules.

3.2.2. VLE of Hexane Isomers. To validate the potential of SAFTD-LJ-Branch being applied to different structures that an alkane isomer may assume, hexane is considered a good choice because it has five isomers. Among the five hexane isomers: *n*-hexane is linear; 2-methylpentane and 3-methylpentane both have one branch but at different carbon positions; 2,3-dimethylbutane has two branches located at different positions on the backbone whereas the two branches of 2,2-dimethylbutane connect to the same carbon atom. Following the argument in section 2.2, it is straightforward to determine the values of NB for each hexane isomer, as is listed in Table 3; the values of parameters m, σ, and ϵ are the same as for *n*-hexane.

As shown in Figure 4, vapor pressures are modeled for each hexane isomer and plotted as a function of reciprocal temperature. Theoretical results match the NIST values[52] well, especially at low temperatures. Note that using SAFTD-LJ-Branch, 2-methylpentane and 3-methylpentane share the same set of parameters and should yield the same results theoretically. Though not identical, the experimental vapor pressures of these two isomers fall very close to each other.

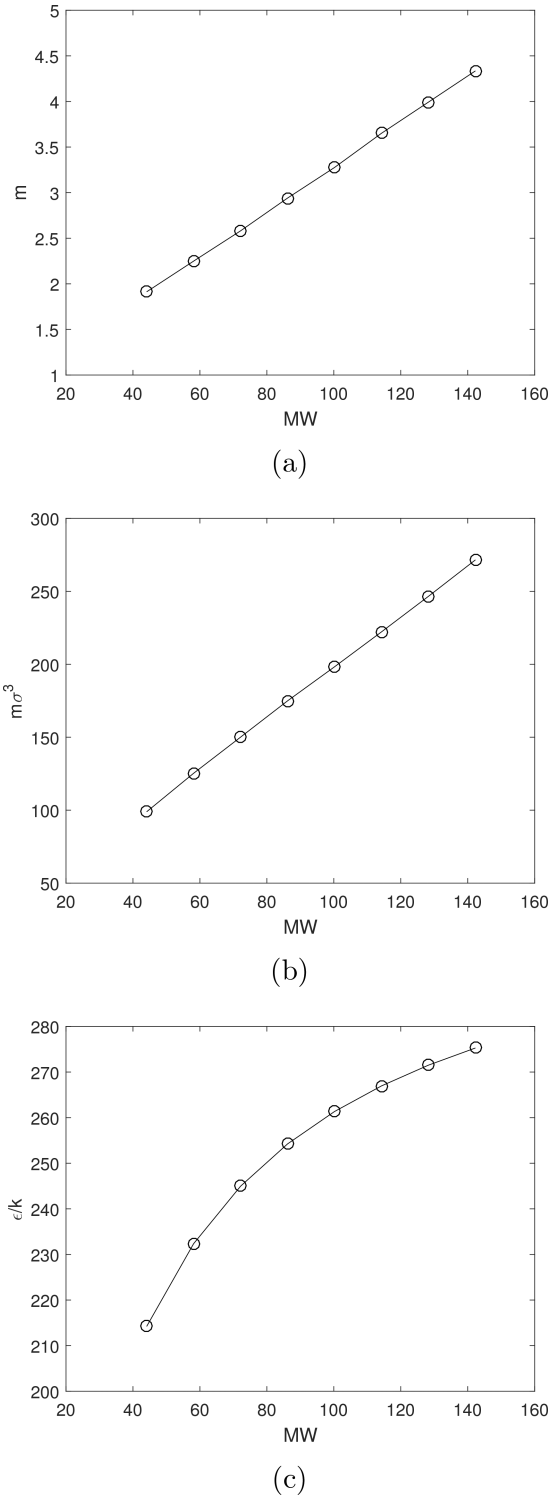

Figure 2. Parameters of SAFTD-LJ EoS for the series of *n*-alkanes, correlated from propane to *n*-decane. Lines are for eye guidance. (a) m as a function of MW. (b) $m\sigma^3$ as a function of MW. (c) ϵ/k as a function of MW.

Saturated densities at different temperatures for each hexane isomer are plotted in Figure 5 and compared against the values of Kay[55] correlated from experiments. The agreement for densities is not as satisfactory as that for vapor pressures. Overall, the theory overestimates the branching effect on the vapor density whereas it underestimates that on the liquid

DOI: 10.1021/acs.iecr.7b03951
Ind. Eng. Chem. Res. 2018, 57, 1679−1688

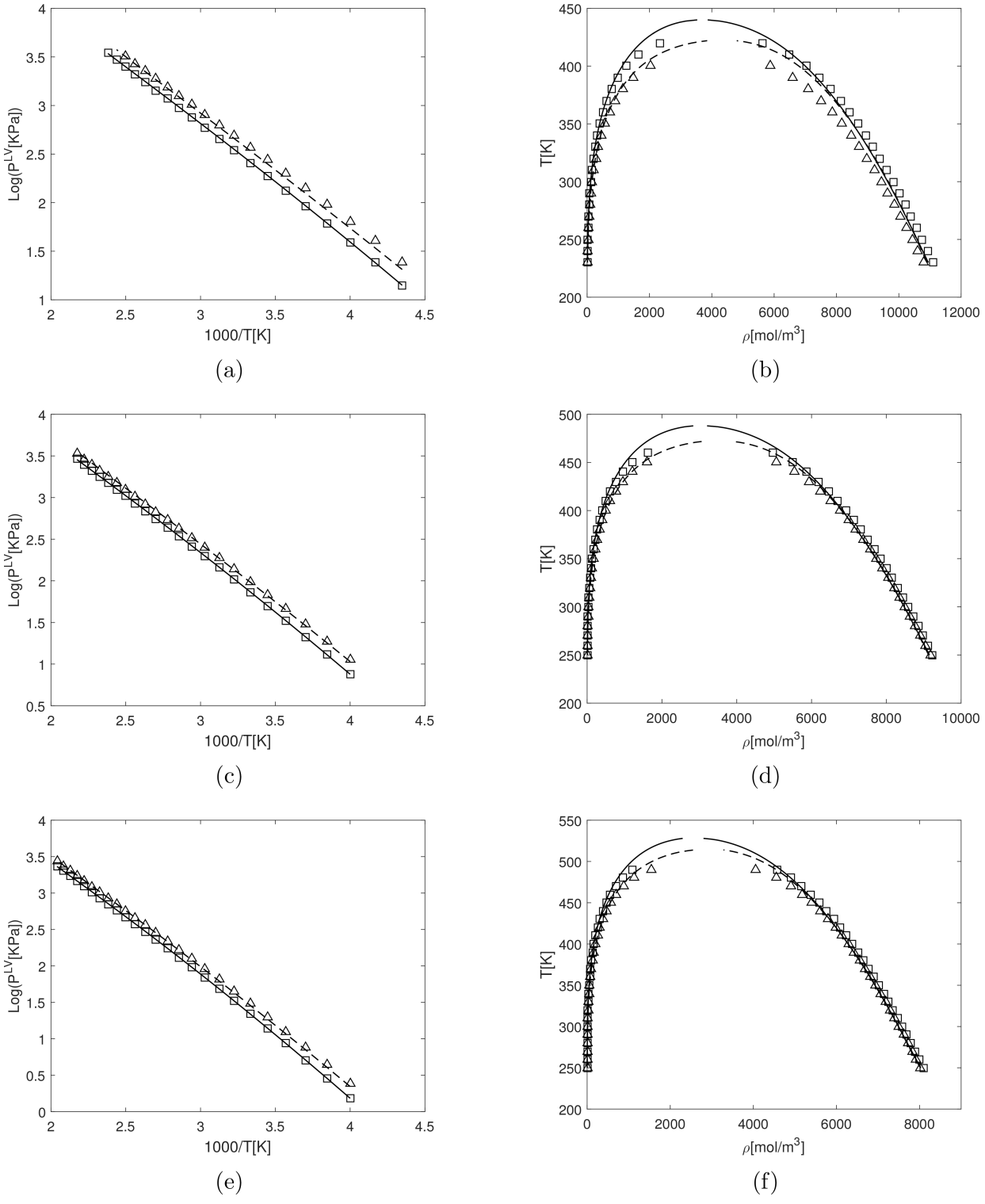

Figure 3. Vapor pressures (a, c, e) and temperature/density coexistence curves (b, d, f) for *n*-butane and isobutane (a, b), *n*-pentane and isopentane (c, d), and *n*-hexane and isohexane (e, f). Squares give NIST values of *n*-alkanes and triangles give NIST values of isoalkanes.[52] Solid lines give theoretical results of *n*-alkanes and dashed lines give theoretical results of isoalkanes.

density. Moreover, 2-methylpentane and 3-methylpentane show non-negligible differences from the correlations, especially for the liquid density. This indicates that more structural information needs to be included to accurately predict densities of isomers with similar extent of branching. For the prediction of vapor pressures, the theory seems to be adequate. The tendency of critical properties for different isomers are found to be consistent with experimental data except for the critical temperature of 2-methylpentane, which is exceptionally low experimentally compared with 2,3-dimethylbutane. The quantitative summary of performance of SAFT-LJ-Branch for different branched hexane isomers is presented in Table 2.

Some may doubt that NB can be determined simply from the structure of hexane because the molecule is modeled as made

DOI: 10.1021/acs.iecr.7b03951
Ind. Eng. Chem. Res. 2018, 57, 1679−1688

Table 2. Performance of SAFTD-LJ-Branch for Pure Components

	AAD (p_V) [%]	AAD (v_L) [%]	T range [K]
isobutane	8.00	3.00	220−387
isopentane	3.55	0.52	230−438
2-methylpentane	3.56	0.45	249−473
3-methylpentane	5.58	1.09	249−359 (p_V), 343−473 (v_L)
2,3-dimethylbutane	13.20	1.35	244−354 (p_V), 343−473 (v_L)
2,2-dimethylbutane	10.33	1.99	237−346 (p_V), 343−463 (v_L)
n-triacontane	14.89	2.54	450−780
squalane	32.51	4.29	450−780

Table 3. Parameters of Different Isomers of Hexane

	m	σ [Å]	ϵ/k [K]	NB
n-hexane	2.941	3.904	253.9	0
2-methylpentane	2.941	3.904	253.9	1
3-methylpentane	2.941	3.904	253.9	1
2,3-dimethylbutane	2.941	3.904	253.9	2
2,2-dimethylbutane	2.941	3.904	253.9	3

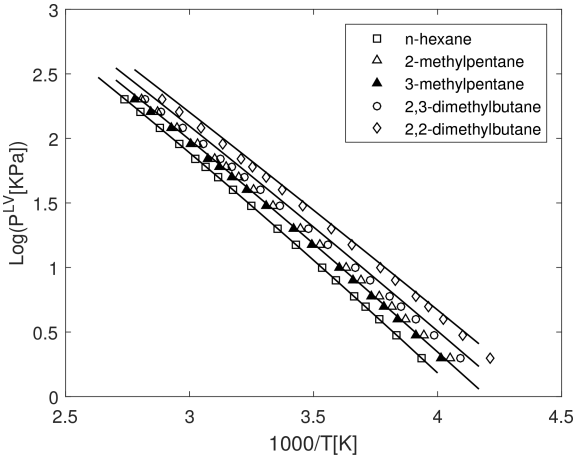

Figure 4. Log base 10 vapor pressures for different isomers of hexane versus reciprocal temperature. Symbols give NIST values[52] and lines are theoretical predictions. Upper lines are of higher NB.

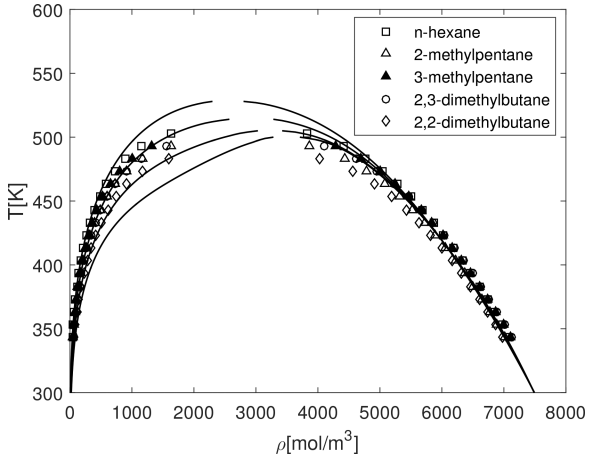

Figure 5. Temperature/density coexistence curves for hexane isomers. Symbols give correlation values of Kay[55] and lines are theoretical predictions. Lower lines are of higher NB.

obtain m = 11.292, σ = 4.069 Å, and ϵ/k = 300.454 K. We use those same numbers for the parameters of squalane with an additional NB = 6. Figure 6 shows the theoretical predictions

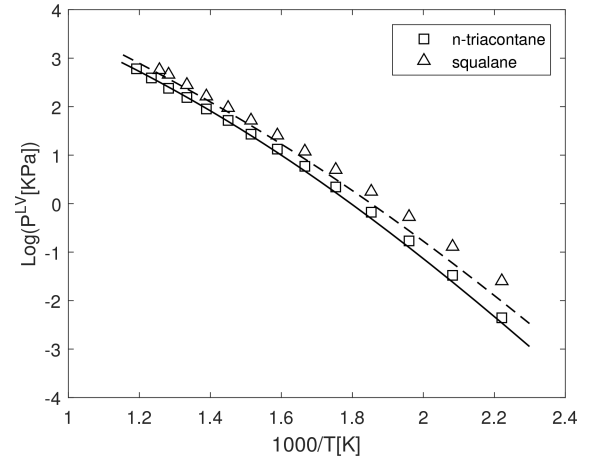

Figure 6. Log base 10 vapor pressures of *n*-triacontane and squalane versus reciprocal temperature. Symbols give NIST values.[52] Solid line gives theoretical results of *n*-triacontane and dashed line gives theoretical results of squalane.

up of 2.941 effective segments (instead of the carbon number in the backbone) and NB should also be an effective branching parameter. For the modeling of 2,2-dimethylbutane, we notice that in Figure 5 the vapor side displays unexpected curvature approaching the critical temperature. We believe that this behavior is a result of the relatively large value of NB (=3) compared with m. Further, we note that a slightly higher or smaller value of NB can improve the agreement with vapor pressure depending on the component. However, because NB assigned this simple way generates encouraging results, we stick to the parameter values in Table 3 for most of this work. We will discuss the role of NB later where it is not necessarily an integer.

3.2.3. VLE of n-Triacontane versus Squalane. In this section we test our theory for heavier alkanes. One chemical of interest is squalane, an isomer of *n*-triacontane. It has six methyl branches almost evenly spread over its backbone. To model *n*-triacontane, we extrapolate the parameters from eq 11 and we for vapor pressures of both *n*-triacontane and squalane, compared aginst values from NIST.[52] We find the theory does a good job in matching the data at high temperatures, particularly because the parameters are extrapolated. At low temperatures, the predicted vapor pressures of both chemicals begin to deviate from the data points with squalane showing a higher deviation. The average absolute deviations for predicted vapor pressures of *n*-triacontane and squalane are 14.89% (maximum is 27.67%) and 32.51% (maximum is 61.71%). These numbers are large partly due to the small values of the true vapor pressures when temperature is low. However, the same direction of deviations observed for both chemicals implies a successful capture of the branching effect.

Due to the unavailability of vapor densities from literature, only the saturated liquid densities of the two isomers are plotted in Figure 7. Contrary to vapor pressures, the theoretical results are more accurate at low temperatures and begin to deviate from NIST values approaching the critical point. There

DOI: 10.1021/acs.iecr.7b03951
Ind. Eng. Chem. Res. 2018, 57, 1679−1688

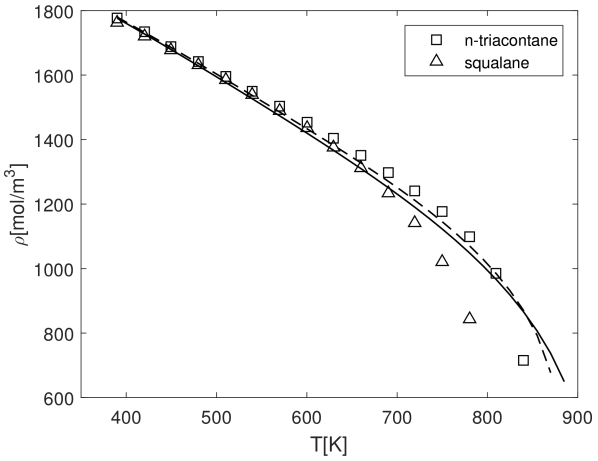

Figure 7. Saturated liquid densities of *n*-triacontane and squalane versus temperature. Symbols give NIST values.[52] Solid line gives theoretical results of *n*-triacontane and dashed line gives theoretical results of squalane.

is little difference between the liquid densities of *n*-triacontane and squalane at low temperatures, and as a matter of fact, the theory incorrectly predicts a slightly higher density for squalane until a crossover at high temperature. The inconsistency may be a result of the parameters extrapolated from short chain alkanes or deficiencies of SAFTD-LJ-Branch itself. The performance of SAFTD-LJ-Branch for *n*-triacontane and squalane is summarized in Table 2.

Despite defects, the results are still inspiring because the parameters are extrapolated from decane and the only required input is the structure of the chemical. This new equation of state provides semiquantitatively accurate predictions of the effect of molecular structure for heavier molecules.

3.3. Phase Equilibrium of Alkane Mixtures. *3.3.1. VLE of Isomeric Hexane and Propane.* We further extend the pure component system to mixtures. Vapor liquid equilibrium of isomeric hexane (using parameters in Table 3) and propane are studied at two temperatures (348.15 and 373.15 K), as shown in Figure 8. For a better look, the system of *n*-hexane and propane is compared against the system of 2/3-methylpentane and propane, system of 2,3-dimethylbutane and propane, system of 2,2-dimethylbutane and propane, respectively. In general, the model gives a good description of the phase equilibrium compared with experimental data[4] and the branching effect is particularly clear for the dew curve. At 373.15 K, the average deviation for the predictions of system of 2,2-dimethylbutane and propane is 1.90% (maximum is 6.13%) in bubble pressure and 12.06% (maximum is 22.34%) in dew pressure. The systems of propane and other hexane isomers behave similarly or better. At low mole fraction of propane, the theory tends to overestimate pressures while at high mole fraction of propane underestimation occurs. However, the overall tendency is nicely captured. With the same composition, the system with more branching (higher NB) features higher dew pressure and bubble pressure, consistent with the pure component case.

3.3.2. Effect of Position Where Branches Grow. In the framework of SAFTD-LJ-Branch, different positions where branches grow are not taken into account as long as the numbers and types of articulation points stay the same. As shown earlier, this was not an issue for mixtures of propane with 2-methylpentane and 3-methylpentane. However, to get

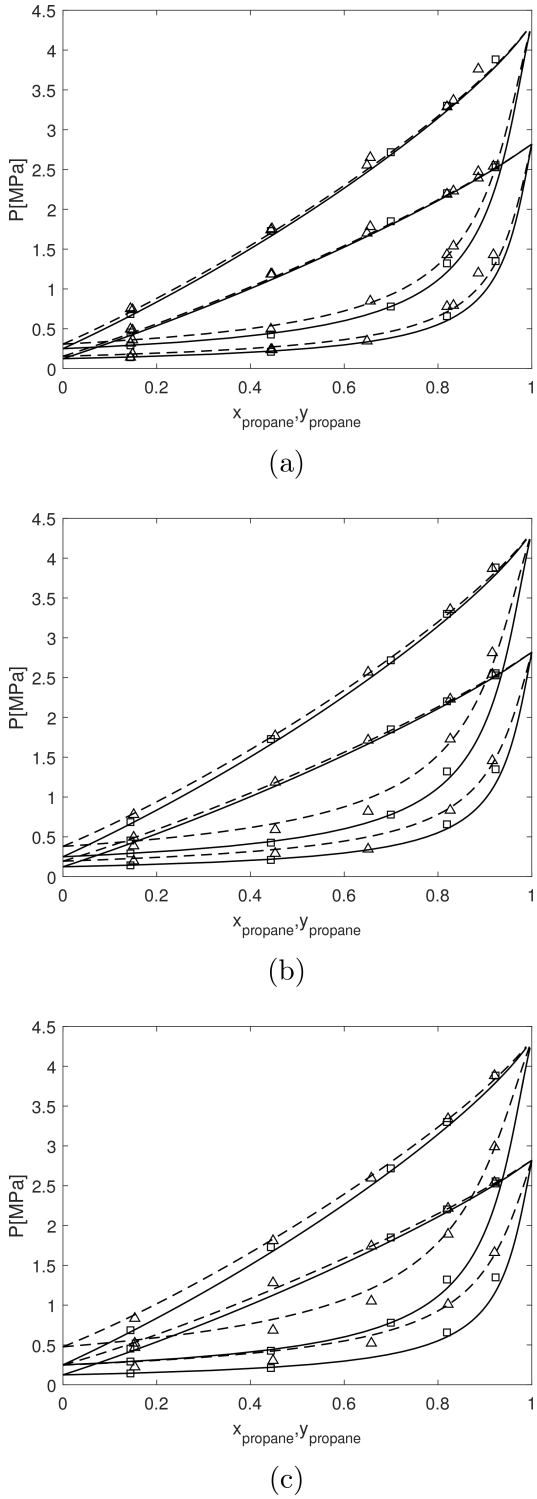

Figure 8. VLE of the mixture propane + isomeric hexane at 348.15 K (lower curver) and 373.15 K (upper curves). In each figure, solid lines are theoretical results for mixture propane + *n*-hexane and dashed lines are theoretical results for mixture propane + branched hexane. Squares give experimental results for mixture propane + *n*-hexane and triangles give experimental results for mixture propane + branched hexane.[4] (a) Comparison with mixture propane + 2/3-methylpentane. (b) Comparison with mixture propane + 2,3-dimethylpentane. (c) Comparison with mixture propane + 2,2-dimethylpentane.

some further insight, this section is devoted to understand the nuances between isomers that only differ in the positions where

DOI: 10.1021/acs.iecr.7b03951
Ind. Eng. Chem. Res. 2018, 57, 1679−1688

branches grow. We model the mixture of 2-methylpentane and *n*-octane as well as the mixture of 3-methylpentane and *n*-octane for vapor liquid equilibrium. The results are shown in Figure 9 and Figure 10. With NB = 1, the theory predicts the

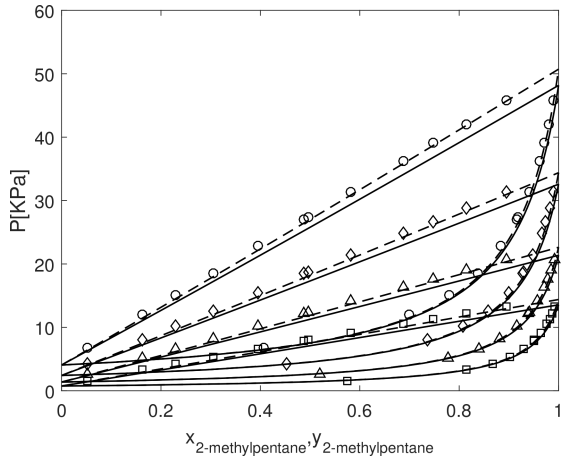

Figure 9. VLE of the mixture 2-methylpentane + *n*-octane at various tmeperatures. Solid lines are theoretical predictions with NB = 1 for 2-methylpentane and dashed lines are theoretical predictions with NB = 1.2 for 2-methylpentane. Symbols are experimental data[3] at 283.15 K (squares), 293.15 K (triangles), 303.15 K (diamomds), and 313.15 K (circles).

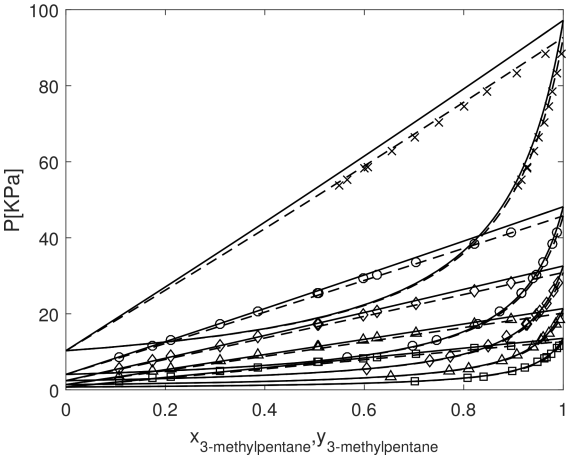

Figure 10. VLE of the mixture 3-methylpentane + *n*-octane at various tmeperatures. Solid lines are theoretical predictions with NB = 1 for 3-methylpentane and dashed lines are theoretical predictions with NB = 0.8 for 3-methylpentane. Symbols are experimental data[3,5] at 283.15 K (squares), 293.15 K (triangles), 303.15 K (diamomds), 313.15 K (circles), and 333.15 K (crosses).

phase behavior well and shows some deviations from experiments[3,5] for both cases. Following the pattern of deviation, we find that a better agreement between prediction and experiments can be obtained when NB is set to around 1.2 for 2-methylpentane and 0.8 for 3-methylpentane. This study is interesting as well as intuitive. 2-Methylpentane has a ternary carbon atom shielded by two methyl groups whereas the ternary carbon atom of 3-methylpentane is surrounded by only one methyl group. A stronger shielding effect for 2-methylpentane leads to a stronger branching effect.

Although the most accurate value for NB is dependent on the system studied, we will not try to fit it nor devise a complicated rule of determination for now. SAFTD-LJ-Branch is developed to provide reasonable solutions to thermodynamics of branched molecules even when no experimental data exist for isomers. We see from the above examples that this model can predict the general trend and provide physically meaningful guidance. In this regard, SAFTD-LJ-Branch is a great tool to study the branched molecules. As we see in the case of 2-methylpentane and 3-methylpentane, NB = 1 tends to be a good average estimate.

In the future, we are interested in a deeper understanding of the relationship between molecular architecture and atoms or groups forming the molecule, potentially leading to better group contribution approaches[56] that explicitly consider molecular architecture.

4. CONCLUSION

This work has a primary focus on thermodynamics of branched molecules. A new equation of state, SAFTD-LJ-Branch is developed through extension of the framework of Marshall and Chapman.[46] The new model is able to predict phase behavior of isomers using a single set of parameters except for the branching parameter, which can be simply obtained from the structure of a molecule. Predictions for pure alkanes and mixtures of alkanes are compared against experimental results with good agreement, especially for the vapor pressures. The accuracy of the predictions is quite surprising considering the simple parametrization scheme and the fact that the branched model adds almost no complexity over the linear model. The theory has strong connections with other popular approaches such as lattice cluster theory and group contribution methods. It also has potential of being applied to associating networks where the effect of branching has been generally neglected.

APPENDIX: EXPRESSION OF A_s^*, $g_s(\sigma)$, AND $g_d(\sigma)$

A_s^* is proposed by Johnson et al.[48] through correlations of simulation results:

$$A_s^* = \frac{A_s}{N_s kT} = \frac{\sum_{i=1}^{8} \frac{a_i \rho_s^{*i}}{i} + \sum_{i=1}^{6} b_i G_i}{T^*} \tag{12}$$

where a_i and b_i are functions of T^* and G_i is a function of ρ_s^*.

The values of g_s and g_d at contact are also fitted from simulation results.[44,49]

$$g_s(\sigma) = 1 + \sum_{i=1}^{5}\sum_{j=1}^{5} a_{ij}(\rho_s^*)^i (T^*)^{1-j} \tag{13}$$

$$g_d(\sigma) = \sum_{i=1}^{7} \hat{a}_i (T^*)^{1-i} + \sum_{i=1}^{5}\sum_{j=1}^{5} c_{ij}(\rho_s^*)^i (T^*)^{1-j} \tag{14}$$

a_{ij}, $\hat{a}_i$, and c_{ij} are all sets of constants. Note that in the reference paper[44] $\hat{a}_i$ is basically a_i. The hat is put here to distinguish from the previous a_i in eq 12.

AUTHOR INFORMATION

Corresponding Author

*W. G. Chapman. E-mail: wgchap@rice.edu.

ORCID

Yuchong Zhang: 0000-0002-6809-1020

Walter G. Chapman: 0000-0002-8789-9041

DOI: 10.1021/acs.iecr.7b03951
Ind. Eng. Chem. Res. 2018, 57, 1679−1688

Notes

The authors declare no competing financial interest.

■ ACKNOWLEDGMENTS

We thank the Robert A. Welch Foundation (Grant No. C-1241) for financial support. We thank Kai Langenbach for his insightful comments and suggestions.

■ REFERENCES

(1) Randic, M. Characterization of molecular branching. *J. Am. Chem. Soc.* **1975**, *97*, 6609−6615.
(2) Yethiraj, A. Integral equation theory for the surface segregation from blends of linear and star polymers. *Comput. Theor. Polym. Sci.* **2000**, *10*, 115−123.
(3) Liu, E. K.; Davison, R. R. Vapor-liquid equilibriums for the binary systems n-octane with 2-methylpentane, 3-methylpentane, and 2, 4dimethylpentane. *J. Chem. Eng. Data* **1981**, *26*, 85−88.
(4) Chun, S. W.; Rainwater, J. C.; Kay, W. B. Vapor-liquid equilibria of mixtures of propane and isomeric hexanes. *J. Chem. Eng. Data* **1993**, *38*, 494−501.
(5) Berro, C.; Laichoubi, F.; Rauzy, E. Isothermal (vapour+ liquid) equilibria and excess volumes of (3-methylpentane+ heptane), of (3-methylpentane+ octane), and of (toluene+ octane). *J. Chem. Thermodyn.* **1994**, *26*, 863−869.
(6) De Loos, T. W.; Poot, W.; Lichtenthaler, R. N. The influence of branching on high-pressure vapor-liquid equilibria in systems of ethylene and polyethylene. *J. Supercrit. Fluids* **1995**, *8*, 282−286.
(7) Freed, K. F. New lattice model for interacting, avoiding polymers with controlled length distribution. *J. Phys. A: Math. Gen.* **1985**, *18*, 871.
(8) Freed, K. F.; Bawendi, M. G. Lattice theories of polymeric fluids. *J. Phys. Chem.* **1989**, *93*, 2194−2203.
(9) Dudowicz, J.; Freed, K. F.; Madden, W. G. Role of molecular structure on the thermodynamic properties of melts, blends, and concentrated polymer solutions. Comparison of Monte Carlo simulations with the cluster theory for the lattice model. *Macromolecules* **1990**, *23*, 4803−4819.
(10) Dudowicz, J.; Freed, K. F. Effect of monomer structure and compressibility on the properties of multicomponent polymer blends and solutions: 1. Lattice cluster theory of compressible systems. *Macromolecules* **1991**, *24*, 5076−5095.
(11) Buta, D.; Freed, K. F.; Szleifer, I. Monte Carlo test of the lattice cluster theory: Thermodynamic properties of binary polymer blends. *J. Chem. Phys.* **2001**, *114*, 1424−1431.
(12) Foreman, K. W.; Freed, K. F. Lattice cluster theory of multicomponent polymer systems: Chain semiflexibility and specific interactions. *Adv. Chem. Physics,* **1998**, *103*, 335−390.
(13) Zeiner, T.; Browarzik, D.; Enders, S. Calculation of the liquid-liquid equilibrium of aqueous solutions of hyperbranched polymers. *Fluid Phase Equilib.* **2009**, *286*, 127−133.
(14) Browarzik, D.; Langenbach, K.; Enders, S.; Browarzik, C. Modeling of the branching influence on liquid-liquid equilibrium of binary and ternary polymer solutions by lattice-cluster theory. *J. Chem. Thermodyn.* **2013**, *62*, 56−63.
(15) Langenbach, K.; Enders, S. Development of an EOS based on lattice cluster theory for pure components. *Fluid Phase Equilib.* **2012**, *331*, 58−79.
(16) Langenbach, K.; Enders, S.; Browarzik, C.; Browarzik, D. Calculation of the high pressure phase equilibrium in hyperbranched polymer systems with the lattice-cluster theory. *J. Chem. Thermodyn.* **2013**, *59*, 107−113.
(17) Fischlschweiger, M.; Enders, S. Solid-liquid equilibria of crystalline and semi-crystalline monodisperse polymers, taking into account the molecular architecture by application of the lattice cluster theory. *Mol. Phys.* **2014**, *112*, 3109−3119.
(18) Langenbach, K.; Browarzik, D.; Sailer, J.; Enders, S. New formulation of the lattice cluster theory equation of state for multi-component systems. *Fluid Phase Equilib.* **2014**, *362*, 196−212.
(19) Langenbach, K.; Fischlschweiger, M.; Enders, S. Prediction of the solid-liquid-liquid equilibria of linear and branched semi-crystalline poly-ethylene in solutions of diphenyl ether by Lattice Cluster Theory. *Mol. Phys.* **2016**, *114*, 2717−2723.
(20) Zimmermann, P.; Goetsch, T.; Zeiner, T.; Enders, S. Modelling of adsorption isotherms of isomers using density functional theory. *Mol. Phys.* **2017**, *115*, 1389.
(21) Chapman, W. G.; Jackson, G.; Gubbins, K. E. Phase equilibria of associating fluids: chain molecules with multiple bonding sites. *Mol. Phys.* **1988**, *65*, 1057−1079.
(22) Chapman, W. G.; Gubbins, K. E.; Jackson, G.; Radosz, M. SAFT: equation-of-state solution model for associating fluids. *Fluid Phase Equilib.* **1989**, *52*, 31−38.
(23) Chapman, W. G.; Gubbins, K. E.; Jackson, G.; Radosz, M. New reference equation of state for associating liquids. *Ind. Eng. Chem. Res.* **1990**, *29*, 1709−1721.
(24) Huang, S. H.; Radosz, M. Equation of state for small, large, polydisperse, and associating molecules. *Ind. Eng. Chem. Res.* **1990**, *29*, 2284−2294.
(25) Huang, S. H.; Radosz, M. Equation of state for small, large, polydisperse, and associating molecules: extension to fluid mixtures. *Ind. Eng. Chem. Res.* **1991**, *30*, 1994−2005.
(26) Wertheim, M. S. Fluids with highly directional attractive forces. I. Statistical thermodynamics. *J. Stat. Phys.* **1984**, *35*, 19−34.
(27) Wertheim, M. S. Fluids with highly directional attractive forces. II. Thermodynamic perturbation theory and integral equations. *J. Stat. Phys.* **1984**, *35*, 35−47.
(28) Wertheim, M. S. Fluids with highly directional attractive forces. III. Multiple attraction sites. *J. Stat. Phys.* **1986**, *42*, 459−476.
(29) Wertheim, M. S. Fluids with highly directional attractive forces. IV. Equilibrium polymerization. *J. Stat. Phys.* **1986**, *42*, 477−492.
(30) Chapman, W. G. Prediction of the thermodynamic properties of associating Lennard-Jones fluids: Theory and simulation. *J. Chem. Phys.* **1990**, *93*, 4299−4304.
(31) Banaszak, M.; Chiew, Y. C.; Radosz, M. Thermodynamic perturbation theory: Sticky chains and square-well chains. *Phys. Rev. E: Stat. Phys., Plasmas, Fluids, Relat. Interdiscip. Top.* **1993**, *48*, 3760.
(32) Gross, J.; Sadowski, G. Perturbed-chain SAFT: An equation of state based on a perturbation theory for chain molecules. *Ind. Eng. Chem. Res.* **2001**, *40*, 1244−1260.
(33) Gross, J.; Sadowski, G. Application of the perturbed-chain SAFT equation of state to associating systems. *Ind. Eng. Chem. Res.* **2002**, *41*, 5510−5515.
(34) Felipe, J.; Vega, L. F. Thermodynamic behaviour of homonuclear and heteronuclear Lennard-Jones chains with association sites from simulation and theory. *Mol. Phys.* **1997**, *92*, 135−150.
(35) Gil-Villegas, A.; Galindo, A.; Whitehead, P. J.; Mills, S. J.; Jackson, G.; Burgess, A. N. Statistical associating fluid theory for chain molecules with attractive potentials of variable range. *J. Chem. Phys.* **1997**, *106*, 4168−4186.
(36) Wertheim, M. S. Thermodynamic perturbation theory of polymerization. *J. Chem. Phys.* **1987**, *87*, 7323−7331.
(37) Phan, S.; Kierlik, E.; Rosinberg, M. L.; Yu, H.; Stell, G. Equations of state for hard chain molecules. *J. Chem. Phys.* **1993**, *99*, 5326−5335.
(38) Marshall, B. D.; Chapman, W. G. Higher order classical density functional theory for branched chains and rings. *J. Phys. Chem. B* **2011**, *115*, 15036−15047.
(39) Ghonasgi, D.; Chapman, W. G. A new equation of state for hard chain molecules. *J. Chem. Phys.* **1994**, *100*, 6633−6639.
(40) Shukla, K. P.; Chapman, W. G. A two-fluid theory for chain fluid mixtures from thermodynamic perturbation theory. *Mol. Phys.* **1998**, *93*, 287−293.
(41) Shukla, K. P.; Chapman, W. G. TPT2 and SAFTD equations of state for mixtures of hard chain copolymers. *Mol. Phys.* **2000**, *98*, 2045−2052.
(42) Dominik, A.; Jain, S.; Chapman, W. G. New Equation of State for Polymer Solutions Based on the Statistical Associating Fluid

DOI: 10.1021/acs.iecr.7b03951
Ind. Eng. Chem. Res. 2018, 57, 1679−1688

Theory (SAFT)- Dimer Equation for Hard-Chain Molecules. *Ind. Eng. Chem. Res.* **2007**, *46*, 5766−5774.
(43) Chang, J.; Sandler, S. I. An equation of state for the hard-sphere chain fluid: theory and Monte Carlo simulation. *Chem. Eng. Sci.* **1994**, *49*, 2777−2791.
(44) Johnson, J. K. Perturbation theory and computer simulations for linear and ring model polymers. *J. Chem. Phys.* **1996**, *104*, 1729−1742.
(45) Blas, F. J.; Vega, L. F. Improved vapor-liquid equilibria predictions for Lennard-Jones chains from the statistical associating fluid dimer theory: Comparison with Monte Carlo simulations. *J. Chem. Phys.* **2001**, *115*, 4355−4358.
(46) Marshall, B. D.; Chapman, W. G. Three new branched chain equations of state based on Wertheim's perturbation theory. *J. Chem. Phys.* **2013**, *138*, 174109.
(47) Rowlinson, J. S.; Swinton, F. *Liquids and liquid mixtures: Butterworths monographs in chemistry*; Butterworth-Heinemann: Boston, 2013.
(48) Johnson, J. K.; Zollweg, J. A.; Gubbins, K. E. The Lennard-Jones equation of state revisited. *Mol. Phys.* **1993**, *78*, 591−618.
(49) Johnson, J. K.; Mueller, E. A.; Gubbins, K. E. Equation of state for Lennard-Jones chains. *J. Phys. Chem.* **1994**, *98*, 6413−6419.
(50) Ghonasgi, D.; Llano-Restrepo, M.; Chapman, W. G. Henry's law constant for diatomic and polyatomic Lennard-Jones molecules. *J. Chem. Phys.* **1993**, *98*, 5662−5667.
(51) Ghonasgi, D.; Chapman, W. G. Prediction of the properties of model polymer solutions and blends. *AIChE J.* **1994**, *40*, 878−887.
(52) Linstrom, P. J.; Mallard, W. G. *NIST Chemistry webbook*; NIST standard reference database No. 69; NIST: Gaithersburg, MD, 2001.
(53) Pedrosa, N.; Vega, L. F.; Coutinho, J. A. P.; Marrucho, I. M. Phase equilibria calculations of polyethylene solutions from SAFT-type equations of state. *Macromolecules* **2006**, *39*, 4240−4246.
(54) Bymaster, A.; Emborsky, C.; Dominik, A.; Chapman, W. G. Renormalization-group corrections to a perturbed-chain statistical associating fluid theory for pure fluids near to and far from the critical region. *Ind. Eng. Chem. Res.* **2008**, *47*, 6264−6274.
(55) Kay, W. B. The vapor pressures and saturated liquid and vapor densities of the isomeric hexanes. *J. Am. Chem. Soc.* **1946**, *68*, 1336−1339.
(56) Fredenslund, A. *Vapor-liquid equilibria using UNIFAC: a group-contribution method*; Elsevier: Amsterdam, 2012.

DOI: 10.1021/acs.iecr.7b03951
Ind. Eng. Chem. Res. 2018, 57, 1679−1688